Dinuclear Molybdenum and Tungsten Complexes with Metal−Metal Triple Bonds Supported by *p-tert*-Butylcalix[4]arene Ligands

Malcolm H. Chisholm,* Kirsten Folting, William E. Streib, and De-Dong Wu

Department of Chemistry and Molecular Structure Center, Indiana University, Bloomington, Indiana 47405

Received May 11, 1999

In hydrocarbon solvents the compounds $M_2(NMe_2)_6$ (M = Mo, W) react with *p-tert*-butylcalix[4]arene, H_4L, to give the complexes $(H_2NMe_2)_2[M_2(\mu,\eta^2,\eta^2\text{-}L)_2]$, **1** (M = Mo, W). In the molecular structure of **1**·4THF, the calix[4]arene ligands span the Mo≡Mo bond of distance 2.193(1) Å in a μ,η^2,η^2 manner such that each Mo atom is coordinated by four phenolic oxygen atoms that lie roughly in a plane with Mo−Mo−O angles that range from 92 to 102°. The calix[4]arene bowl encapsulates the H_2NMe_2 cations tightly as judged by ^{1}H NMR spectroscopy, and heating to 100 °C under a dynamic vacuum in the solid state fails to remove $HNMe_2$. However, upon refluxing in pyridine, compounds **1** are converted to $(H_2NMe_2)_2[M_2(\eta^4\text{-}L)_2]\cdot x$py, **2**·*x*py. The molecule of **2**·4py (M = Mo) has a center of symmetry, and the Mo_2−calix[4]arene unit has a dumbbell shape (Mo≡Mo bond distance 2.226(1) Å). Each Mo atom has four Mo−O phenoxide bonds, one of which is hydrogen-bonded to a H_2NMe_2 cation, which in turn is hydrogen-bonded to a pyridine molecule. Each calix[4]arene bowl encapsulates one molecule of pyridine. Heating compounds **2** under a dynamic vacuum at 100 °C for 3 days forms compounds **3** of formula $M_2(\eta^4\text{-}HL)_2$. A partial crystal structure determination of **3**·*x*C_6H_6 (M = Mo) revealed Mo≡Mo bonds, 2.226(6) and 2.214(7) Å, supported by η^4-HL ligands. Compounds **3** are formed directly in the reactions between $M_2(O^tBu)_6$ compounds and H_4L in benzene at room temperature (1 or 2 days). Compounds **3** react in hydrocarbon solutions with $HNMe_2$ to give the compounds $(H_2NMe_2)_2[M_2(\eta^4\text{-}L)_2]$, **2**. For tungsten, **3** and **2** react in benzene to give $(H_2NMe_2)[W_2(\eta^4\text{-}L)(\eta^4\text{-}HL)]$, **4**, which crystallizes with seven molecules of benzene, two of which are encapsulated in the calix[4]arene bowls. The W≡W bond, 2.304(1) Å, is spanned by one H_2NMe_2 cation that hydrogen-bonds to a pair of phenolic oxygen atoms while another pair of oxygen atoms in the trans position are directly hydrogen-bonded such that a short O···O distance results, 2.338(9) Å. The monomethylated *p-tert*-butylcalix[4]arene, $H_3L(1)$, reacts with $Mo_2(NMe_2)_6$ to give **3**, $HNMe_2$, and Me_3N whereas $Mo_2(O^tBu)_6$ and $H_3L(1)$ yield $Mo_2(\eta^4\text{-}L(1))_2$, **5**, and ^{t}BuOH. The dimethylated *p-tert*-butylcalix[4]arene, $H_2L(2)$, failed to react with either $Mo_2(NMe_2)_6$ or $Mo_2(O^tBu)_6$ even under prolonged reflux. These results are discussed in terms of the mechanisms of substitution and isomerization reactions of M≡M complexes and are compared with known reactions involving chelating biphenoxides and the coordination chemistry of calix[4]arene ligands.

Introduction

Compounds with multiple bonds between metal atoms form an important class of compounds in nontraditional coordination chemistry.[1] The structures, bonding, and attendant spectroscopies have attracted much attention over the past three decades since the discovery of the M−M quadruple bond in the $Re_2Cl_8^{2-}$ anion. Much less is known, however, about the details of their reaction chemistry, though many interesting reactions are known.[2] Even the fundamental aspects of their substitution chemistry have been largely ignored save for establishment of stoichiometry. We are currently investigating whether some basic principles of reaction pathways can be correlated with the ground-state electronic structures of these complexes.[3]

Some time ago, we noted that, starting from the complex $1,2\text{-}Mo_2Br_2(CH_2SiMe_3)_4$, one could prepare $Mo_2(NMe_2)_2(CH_2SiMe_3)_4$ as either one of two isomers shown in **A** and **B**.[4] Moreover, these isomers did not interconvert in benzene-d_6 even at 100 °C.

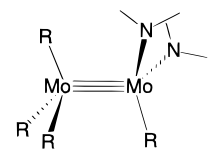

A

$1,1\text{-}Mo_2(NMe_2)_2(CH_2SiMe_3)_4$

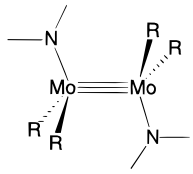

B

$1,2\text{-}Mo_2(NMe_2)_2(CH_2SiMe_3)_4$

The high barrier to interconversion of 1,1- and 1,2-isomers indicates bridged intermediates are not readily accessible for these so-called "ethane-like dimers".[5] Subsequent work reinforced this notion and showed that ligand association was necessary to promote interconversion of 1,1- and 1,2-isomers as in the reaction shown in eq 1.[6] Furthermore only in the case

(1) Cotton, F. A.; Walton, R. A. *Multiple Bonds between Metal Atoms*, 2nd ed.; Oxford University Press: Oxford, U.K., 1993.
(2) Review of ref 1 by: Williams, A. F. *Angew. Chem., Int. Ed. Engl.* **1994**, *33*, 480.
(3) (a) Casas, J. M.; Cayton, R. H.; Chisholm, M. H. *Inorg. Chem.* **1991**, *30*, 358. (b) Chisholm, M. H.; McInnes, J. M. *J. Chem. Soc., Dalton Trans.* **1997**, 2735 and references therein.
(4) Chisholm, M. H.; Folting, K.; Huffman, J. C.; Rothwell, I. P. *Organometallics* **1982**, *1*, 251.
(5) Chisholm, M. H. *Acc. Chem. Res.* **1990**, *23*, 419.
(6) Chisholm, M. H.; Folting, K.; Huffman, J. C.; Kramer, K. S.; Tatz, R. J. *Organometallics* **1992**, *11*, 4029.

10.1021/ic990513a CCC: $18.00
Published on Web 10/20/1999

of attendant phosphido ligands have we ever seen an equilibrium between open and bridged isomers, eq **2**.[7]

$$1,2\text{-}Mo_2(CH_2Ph)_2(O^iPr)_4 + PMe_3 \rightleftharpoons 1,1\text{-}Mo_2(CH_2Ph)_2(O^iPr)_4(PMe_3) \quad (1)$$

$$1,2\text{-}W_2(PR_2)_2(NMe_2)_4 \rightleftharpoons W_2(\mu\text{-}PR_2)_2(NMe_2)_4 \quad (2)$$

In solution, all the reactions of $M_2(NMe_2)_6$ and $M_2(OR)_6$ compounds (M = Mo, W) proceed by an associative pathway, and in one instance, we have observed the reversible self-association reaction shown in eq 3,[8] which yields a 12-electron cluster, an inorganic analogue of cyclobutadiene.[9]

$$2[W_2(O^iPr)_6] \rightleftharpoons W_4(O^iPr)_{12} \quad (3)$$

Bidentate ligands may provide further mechanistic information concerning reaction pathways for these compounds because of (i) the chelate effect and (ii) the inertness of the products. In this manner, we have elucidated kinetic and thermodynamic aspects of substitution reactions employing diols[10] and sterically encumbered phenols of the types shown in **C** and **D**.[11]

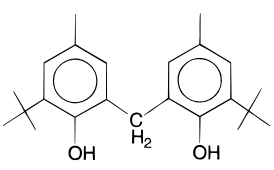

C

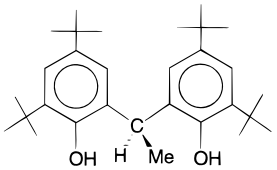

D

Typically bridged isomers are formed as kinetic products where the biphenoxide spans the M−M bond with a nine-membered ring. In the presence of a Lewis base such as pyridine, these isomerize to the chelate isomer with eight-membered rings, as shown schematically in eq 4.[11]

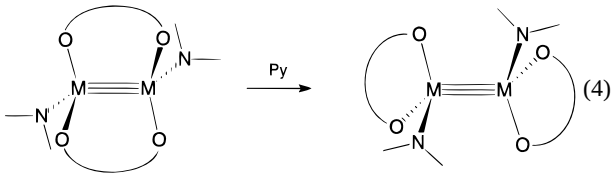

(4)

Reaction 4, when carried out in benzene-d_6, was shown to be second order in pyridine, which led us to propose a symmetrical intermediate or transition state of the type shown in **E**.[11a]

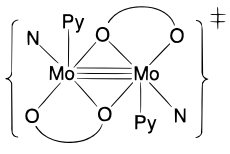

E

We turn here to the use of the *p-tert*-butylcalix[4]arene ligand. The bowl-like calix[*n*]arene molecules have attracted much attention in terms of host−guest and molecular recognition chemistry,[12] and for the sake of simplicity we represent the free ligand as shown in **F**.

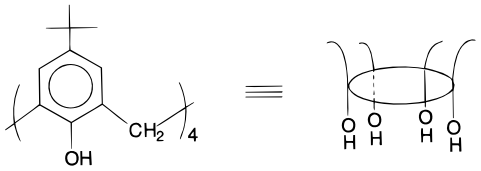

F

The drawing in **F** emphasizes the relationship between the biphenoxides, **C** and **D**, and the calix[4]arene ligand. In addition, we have studied the reactions involving the partially methylated calix[4]arenes,[13] referred to as $H_3L(1)$ and $H_2L(2)$ for brevity and shown in the drawings **G** and **H**. At this time, the most

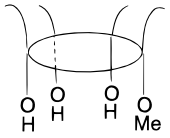

G

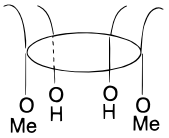

H

relevant work involving the coordination chemistry of calix[4]-arene, especially with dinuclear centers, comes from the independent work of Lippard[14] and Floriani.[15] We shall refer to this in detail as we present our findings.

Results and Discussion

Syntheses. Benzene solutions of $M_2(NMe_2)_6$ react with 2 equiv of *tert*-butylcalix[4]arene, H_4L, at room temperature for M = Mo and under reflux for M = W to give the compounds $(H_2NMe_2)_2[M_2(\mu,\eta^2,\eta^2\text{-}L)_2]$, **1**, which are green and were crystallized from THF as THF solvates. In the preparation of **1**, it is desirable to use slightly less than 2 equiv of the calix-[4]arene ligand because **1** is easily separable from unreacted $M_2(NMe_2)_6$ by washing with hexane. [Hexane readily dissolves the more soluble $M_2(NMe_2)_6$ compounds.] It is also worthy of mention that, with only 1 equiv of H_4L, compounds **1** and unreacted $M_2(NMe_2)_6$ are formed. We have found no evidence for a partially substituted compound.

Compounds **1** react in refluxing pyridine to form $(H_2NMe_2)_2$-$[M_2(\eta^4\text{-}L)_2]$, **2**, which upon crystallization yield $(H_2NMe_2)_2[M_2$-$(\eta^4\text{-}L)_2]\cdot x$py, **2**·*x*py. The molybdenum compound is amber while the tungsten compound is green, similar to the color of **1** (M = W). Heating the pyridine solvate complexes **2**·*x*py under a dynamic vacuum for 3 days results in the formation of compounds **3**, which are brown (M = Mo, W) and soluble in benzene and toluene. The formulas for **3** are represented by M_2-$(\eta^4\text{-}HL)_2$, and these compounds can be prepared directly from the reaction between $M_2(O^tBu)_6$ compounds and H_4L (<2 equiv).

(7) Buhro, W. E.; Chisholm, M. H.; Folting, K.; Huffman, J. C.; Martin, J. D.; Streib, W. E. *J. Am. Chem. Soc.* **1988**, *110*, 6563.
(8) Chisholm, M. H.; Clark, D. L.; Hampden-Smith, M. J. *J. Am. Chem. Soc.* **1989**, *111*, 574.
(9) Chisholm, M. H.; Clark, D. L.; Folting, K.; Huffman, J. C.; Hampden-Smith, M. J. *J. Am. Chem. Soc.* **1987**, *109*, 7750.
(10) Chisholm, M. H.; Parkin, I. P.; Folting, K.; Lobkovsky, E. *Inorg. Chem.* **1996**, *36*, 1636.
(11) (a) For **C**: Chisholm, M. H.; Huang, J.-H.; Huffman, J. C.; Parkin, I. P. *Inorg. Chem.* **1997**, *37*, 11642. (b) For **D**: Chisholm, M. H.; Folting, K.; Streib, W. E.; Wu, D.-D. *Inorg. Chem.* **1998**, *38*, 50.
(12) (a) Gutsche, C. D. *Calixarenes*; The Royal Society of Chemistry: Cambridge, U.K., 1989; Vol. 1. (b) Atwood, J. L.; Orr, G. W.; Juneja, R. K.; Bott, S. G.; Hamada, F. *Pure Appl. Chem.* **1993**, *65*, 1471.
(13) Zanotti-Gerosa, A.; Solasi, E.; Giannini, L.; Floriani, C.; Re, N.; Chiesi-Villa, A.; Rizzoli, C. *Inorg. Chim. Acta* **1998**, *270*, 298.
(14) (a) Acho, A J.; Lippard, S. J. *Inorg. Chim. Acta* **1995**, *229*, 5. (b) Acho, J. A.; Ren, T.; Yun, J. W.; Lippard, S. J. *Inorg. Chem.* **1995**, *34*, 5226.
(15) (a) Giannini, L.; Solari, E.; Zanotti-Gerosa, A.; Floriani, C.; Chiesi-Villa, A.; Rizzoli, C. *Angew. Chem., Int. Ed. Engl.* **1997**, *36*, 753. (b) Zanottii-Gerosa, A.; Solari, E.; Giannini, L.; Floriani, C.; Chiesi-Villa, A.; Rizzoli, C. *J. Am. Chem. Soc.* **1998**, *120*, 437.

Scheme 1[a]

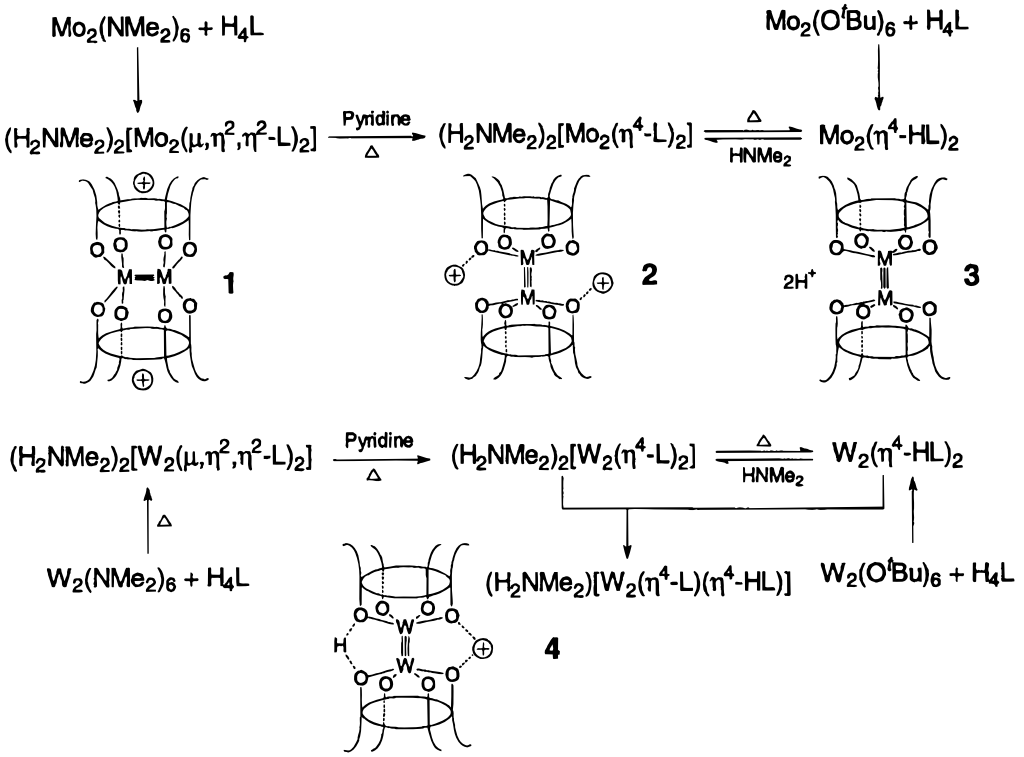

[a] ⊕ = $H_2NMe_2^+$.

The addition of $HNMe_2$ to benzene solutions of **3** yields yellow (M = Mo) and pale green (M = W) precipitates, $(H_2NMe_2)_2[M_2(\eta^4\text{-L})_2]$, **2**, which upon addition of pyridine yield **2**·*x*py.

For tungsten, but not molybdenum, the compounds $(H_2NMe_2)_2[M_2(\eta^4\text{-L})_2]$, **2** (M = W), and $M_2(\eta^4\text{-HL})_2$, **3** (M = W), react in benzene to give $(H_2NMe_2)[W_2(\eta^4\text{-L})(\eta^4\text{-HL})]$, **4**, which is pale green and yields a benzene solvate crystalline compound, **4**·7HPh.

These reactions are summarized in Scheme 1. The reaction between $Mo_2(NMe_2)_6$ and the monomethylated calix[4]arene ligand $H_3L(1)$ (shown in **G**) proceeds to give compound **2** (M = Mo) according to the stoichometry shown in eq 5. However,

$$Mo_2(NMe_2)_6 + 2H_3L(1) \xrightarrow[\text{benzene}]{60\ ^\circ\text{C}} (Me_2NH_2)_2Mo_2(\eta^4\text{-L})_2 + 2Me_2NH + 2Me_3N \quad (5)$$

the reaction involving $Mo_2(O^tBu)_6$ and $H_3L(1)$ proceeds to give $Mo_2(\eta^4\text{-L}(1))_2$, **5**, and ^{t}BuOH. These reactions involving H_3L-(1) are shown in Scheme 2. It is of note that the reaction employing the dimethylamide proceeds in this instance directly to the η^4-L bonding mode. No η^2,η^2-L bonding was observed. Also, the reaction employing the dimethylamide leads to loss of the methyl group with formation of Me_3N whereas, in the O^{t}Bu substitution reaction, the OMe moiety is retained in the product $Mo_2(\mu^4\text{-L}(1))_2$, **5**.

Attempted reactions between the dimethylated calix[4]arene, $H_2L(2)$, shown in **H**, failed inasmuch as both $Mo_2(NMe_2)_6$ and $Mo_2(O^tBu)_6$ were recovered unreacted both from attempted reactions in solution with heating and even from solid-state reactions at 180 °C. This is clear evidence for a significant kinetic barrier to substitution by the $H_2L(2)$ ligand at the Mo_2^{6+} center.

The crystalline molybdenum compounds are relatively air-stable while the tungsten analogues are not. The new compounds have been characterized by infrared and ^{1}H and ^{13}C{^{1}H} NMR spectroscopy and by single-crystal X-ray crystallography. For brevity, we present the X-ray molecular structural information first and then correlate this with solution behavior.

Single-Crystal and Molecular Structures. $(H_2NMe_2)_2$-$[M_2(\mu,\eta^2,\eta^2\text{-L})_2]\cdot 4THF$, 1, where M = Mo and W, are isostructural, but the molecular structure was only solved for M = Mo. Although there were some crystallographic problems associated with this structure (as outlined in the Experimental Section and in the CIF files of the Supporting Information), the essential features of the structure are known beyond any doubt.

An ORTEP drawing of **1** (M = Mo) is shown in Figure 1. The calix[4]arene ligand spans the Mo≡Mo bond of distance 2.194(2) Å. The M−O distances range from 1.95 to 2.03 Å, and the H_2NMe_2 cation is encapsulated within the calix[4]arene bowl. Each Mo atom is coordinated to four oxygen atoms that lie roughly in a square plane, with the Mo−Mo−O angles falling between 92 and 102°. A view down the M−M axis is shown in Figure 2, and this reveals that the central Mo_2O_8 unit is staggered and not eclipsed. Inasmuch as the calix[4]arene ligand can be viewed a two cojoined methylene biphenoxides of the type we have previously studied in $M_2(NMe_2)_2(O{\sim\sim}CH_2{\sim\sim}O)_2$ complexes,[11] this noneclipsed geometry might have been anticipated. The Mo−O distances are somewhat shorter than those reported for the μ,η^2,η^2-calix[4]arene ligand coordinated to the Mo_2^{4+} center,[14] as would be expected on the basis of charge and O pπ to Mo dπ bonding.[16]

The encapsulated H_2NMe_2 cation does not appear to be strongly hydrogen-bonded to any of the oxygen atoms, as the shortest O···N distance is 3.1 Å. Also, from an inspection of Figure 1, one sees that the phenyl rings are in a pairwise manner disposed in and out, with those out being related to the shortest O···N distances. It seems probable that the *N*-methyl groups

(16) Chisholm, M. H.; Folting, K.; Huffman, J. C.; Putilina, E. F.; Streib, W. E.; Tatz, R. J. *Inorg. Chem.* **1993**, *32*, 3771.

Scheme 2[a]

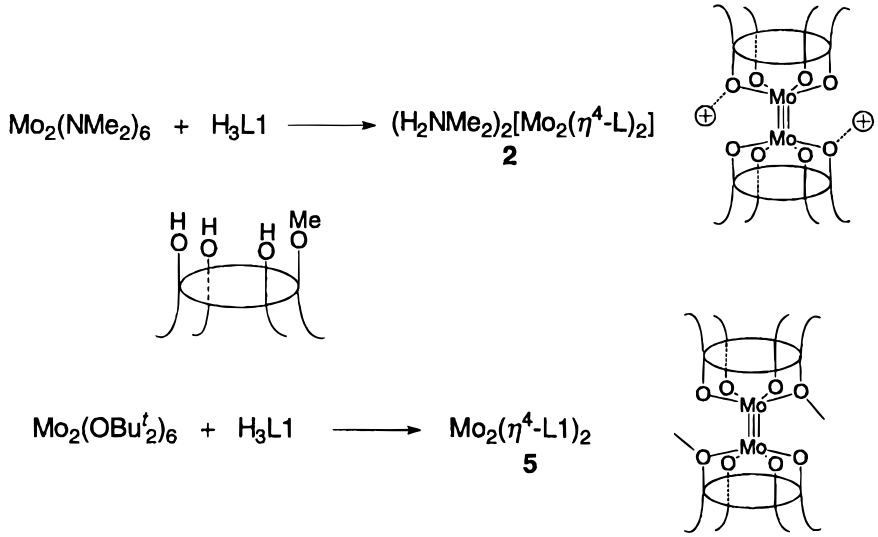

[a] $\oplus = H_2NMe_2^+$.

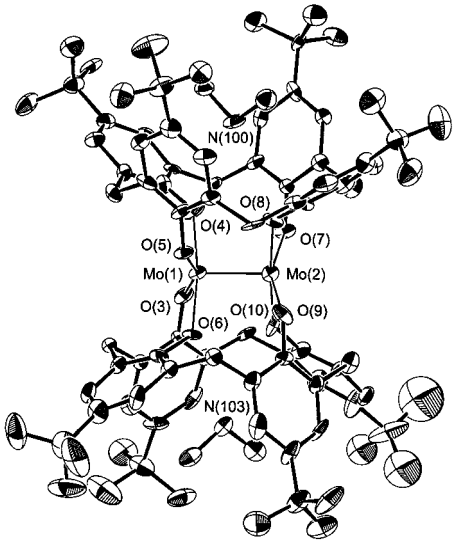

Figure 1. ORTEP drawing of **1** (M = Mo), with the atom-numbering scheme, showing the coordination geometry of metal atoms.

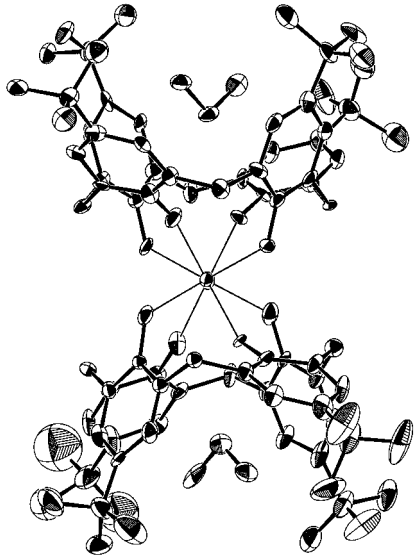

Figure 2. ORTEP drawing of **1** (M = Mo) showing the staggered conformation of the central Mo_2O_8 unit.

interact with a pair of trans phenyl groups to cause the opening of the bowl. One can also argue that the positive charge of the H_2NMe_2 protons (N−H) causes a favorable N−H···phenyl interaction such that two of the H_2NMe_2 nitrogen atoms are closer to the central Mo_2 moiety in **1** (M = Mo) than are the pyridine nitrogen atoms in the structures to be discussed shortly. The geometry of the calix[4]arene ligands in **1** contrasts with that reported by Lippard and co-workers for $Mo_2(OAc)_2(\mu,\eta^2,\eta^2\text{-}H_2L)$, which has effective 4-fold symmetry.[14]

Finally it is worth noting that the THF molecules are not within the coordination environment of the Mo_2^{6+} unit. Selected bond distances and bond angles are given in Table 1.

$(H_2NMe_2)_2[Mo_2(\eta^4\text{-}L)_2]\cdot 4py$, 2 (M = Mo). A view of the molecular structure of **2** is given in Figure 3. The dumbbell-like structure again contains two four-coordinate Mo atoms, with Mo−O distances spanning the narrow range 1.97−2.03 Å and Mo−Mo−O angles spanning the range 97−100°. The Mo−Mo distance of 2.226(1) Å is slightly longer than that in **1** but typical of a Mo−Mo triple-bond distance in $Mo_2(OR)_6$ compounds and related adducts such as $Mo_2(O^iPr)_6(HNMe_2)_2$.[1,17] The Mo_2O_8 skeleton is essentially eclipsed in **2**.

Table 1. Selected Bond Distances (Å) and Angles (deg) for **1**·4THF (M = Mo)

Mo1−Mo2	2.193(1)	Mo1−O3	2.029(7)
Mo1−O4	1.958(7)	Mo1−O5	2.009(7)
Mo1−O6	1.964(7)	Mo2−O7	2.027(7)
Mo2−O8	1.994(7)	Mo2−O9	2.021(7)
Mo2−O10	1.960(8)		
O10−Mo2−Mo1	92.7(2)	O8−Mo2−Mo1	92.2(2)
O9−Mo2−Mo1	100.9(2)	O7−Mo2−Mo1	102.2(2)
O4−Mo1−Mo2	93.8(2)	O6−Mo1−Mo2	94.4(2)
O5−Mo1−Mo2	102.0(2)	O3−Mo1−Mo2	101.2(2)
O4−Mo1−O6	171.8(3)	O4−Mo1−O5	88.8(3)
O6−Mo1−O5	89.0(3)	O4−Mo1−O3	92.3(3)
O6−Mo1−O3	86.7(3)	O5−Mo1−O3	156.7(3)
O10−Mo2−O8	175.1(3)	O10−Mo2−O9	88.1(3)
O8−Mo2−O9	90.8(3)	O10−Mo2−O7	91.9(3)
O8−Mo2−O7	87.2(3)	O9−Mo2−O7	156.9(3)

A particularly interesting feature of the structure is that the H_2NMe_2 cation is hydrogen-bonded to one oxygen of the calix-[4]arene ligand and to a pyridine molecule. The hydrogen atoms

(17) Chisholm, M. H. *Polyhedron* **1983**, *2*, 681.

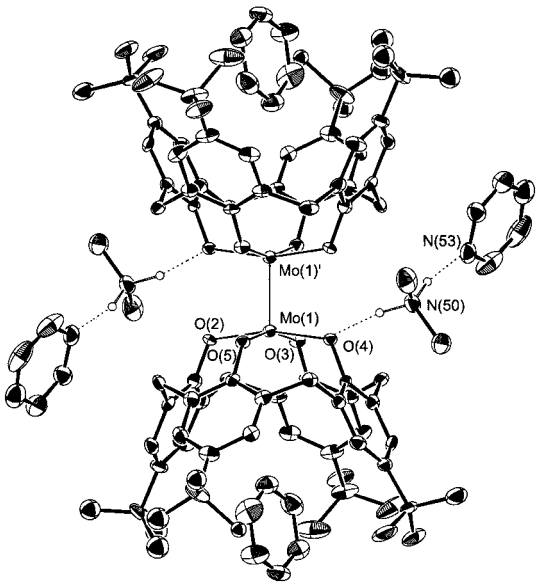

Figure 3. ORTEP drawing of **2**·4py (M = Mo), with the atom-numbering scheme, showing the dumbbell-like structure and hydrogen bonding. The molecule has a crystallographically imposed inversion center.

Table 2. Selected Bond Distances (Å) and Angles (deg) for **2**·4Py (M = Mo)

Mo1−Mo1	2.226(1)	Mo1−O2	2.009(4)
Mo1−O3	1.975(4)	Mo1−O4	2.028(4)
Mo1−O5	1.973(4)		
N50···O4	2.856(7)	N50···N53	2.804(8)
Mo1−Mo1−O2	97.9(1)	Mo1−Mo1−O3	98.8(1)
Mo1−Mo1−O4	97.1(1)	Mo1−Mo1−O5	100.1(1)
O2−Mo1−O3	89.2(2)	O2−Mo1−O4	165.1(2)
O2−Mo1−O5	89.1(2)	O3−Mo1−O4	88.2(2)
O3−Mo1−O5	161.2(2)	O4−Mo1−O5	88.6(2)

were located in the structural determination of **2**, and the NH···N interactions are shown in Figure 3. The Mo1−O4 distance of 2.028(4) Å is the longest Mo−O distance as a result of this hydrogen bonding. A similar situation is seen in the sodium, Na^+, bridged complex $[\mu\text{-Na}]_2[W_2(\eta^4\text{-L})_2]$ reported by Floriani.[15a]

It can also be seen from an inspection of Figure 3 that a molecule of pyridine is partially encapsulated by each calix[4]-arene bowl. The position of the nitrogen atom in this pyridine molecule is not known. In terms of the refinement, it was chosen to be 50:50 in and out, but in reality it could be averaged over all six positions of the ring. In contrast to **1**, the calix[4]arene ligand has virtual C_4 symmetry. Selected bond distances and angles are given in Table 2.

$[Mo_2(\eta^4\text{-HL})_2]$·*x*HPh, 3 (M = Mo). The structural determination of **3**, though not crystallographically satisfactory, is offered here because it confirms the dumbbell-like structure for **3** (the latter is demanded by NMR data presented later). In the crystal, there are two independent molecules, each having unusually high crystallographically imposed symmetry. The two independent molecules have very similar Mo−Mo triple-bond distances, 2.21(1) and 2.23(1) Å. In one molecule, there is only one M−O distance, 1.97(1) Å, while in the other, there are two, 1.95(2) and 2.11(3) Å. A view of the molecule having D_{4d} symmetry is shown in Figure 4.

The location of the two hydrogen atoms required for charge balance for the Mo_2^{6+} central moiety cannot be established from the structure. However, it is reasonably assumed to be bridging

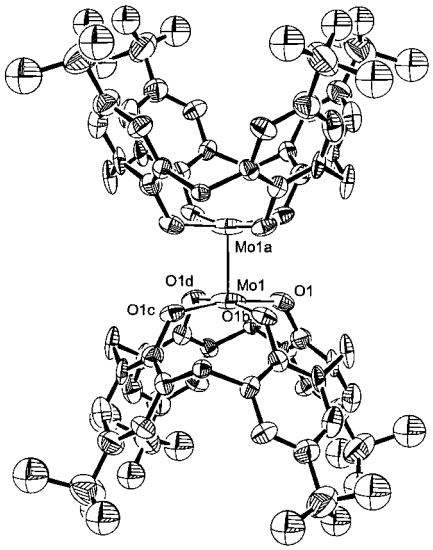

Figure 4. ORTEP drawing of **3** (M = Mo), with the atom-numbering scheme, showing the dumbbell-like structure. The molecule has crystallographically imposed D_{4d} symmetry.

Table 3. Selected Bond Distances (Å) and Angles (deg) for **3**·*x*HPh (M = Mo)

Mo1−Mo1	2.226(6)	Mo1−O1	1.97(1)
Mo2−Mo2	2.214(7)	Mo2−O2	2.11(3)
Mo2−O3	1.95(2)		
O1···O1	2.62(3)	O2···O2	2.66(3)
O3···O3	2.74(3)		
O1−Mo1−Mo1	95.8(3)	O1−Mo1−O1	88.5(6)
O1−Mo1−O1	90.3(6)	O1−Mo1−O1	168.4(6)
O3−Mo2−Mo2	97.7(4)	O2−Mo2−Mo2	96.1(6)
O3−Mo2−O3	164.6(8)	O3−Mo2−O2	89.2(1)
O2−Mo2−O2	168(1)		

two oxygen atoms across the Mo−Mo bond, and this is supported by ^{1}H NMR data presented later. Also the interligand O···O distances range from 2.62(3) to 2.74(3) Å.

Selected bond distances and angles for the two molecules are given in Table 3.

$(H_2NMe_2)[W_2(\eta^4\text{-L})(\eta^4\text{-HL})]$·7HPh, 4 (M = W). A unit cell drawing of this structure is shown in Figure 5, which reveals both the packing of the dumbbell-like molecules and the ordering of the benzene molecules. Each calix[4]arene bowl has a partially encapsulated benzene, while five others are arranged around the girth of the Mo−Mo triple bonds.

A diagram of the molecular structure of **4**, viewed perpendicular to the W−W axis and omitting the benzene molecules for clarity, is given in Figure 6. The molecule has a crystallographic mirror plane of symmetry, one H_2NMe_2 cation, and one H^+ link opposite oxygen atoms by hydrogen bonding. The O2···H···O2′ distance is 2.338(9) Å, notably shorter than the other O···O distances. The W_2O_8 unit is eclipsed with W−O distances spanning the range 1.95(1)−2.07(1) Å. The longer distances are involved in hydrogen bonding. The W−W−O2 angle is 90.5(2)° while the W−W−O4 angle is 102.8(2)° as a result of the bridging H^+ and $H_2NMe_2^+$ ions, respectively. Again, a certain similarity can be seen with the $[\mu\text{-Na}]_2[W_2(\eta^4\text{-L})_2]$ structure reported by Floriani[15a] in terms of W−O distances and W−W−O angles.

Selected bond distances and angles are given in Table 4, and a summary of the crystallographic data for the four compounds described herein is given in Table 5.

Spectroscopic Characterizations. Compounds **1** show interesting variable-temperature NMR spectra which can be

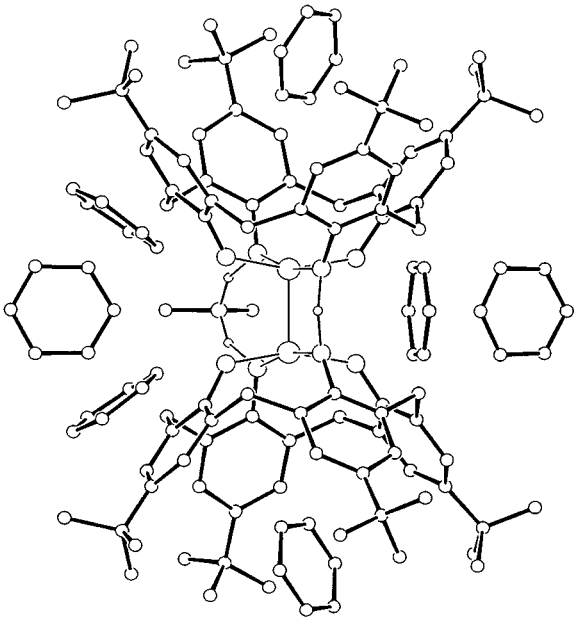

Figure 5. Molecular drawing of **4**·7PhH (M = W) showing the ordering of the solvate benzene molecules. The molecule has a crystallographically imposed mirror plane.

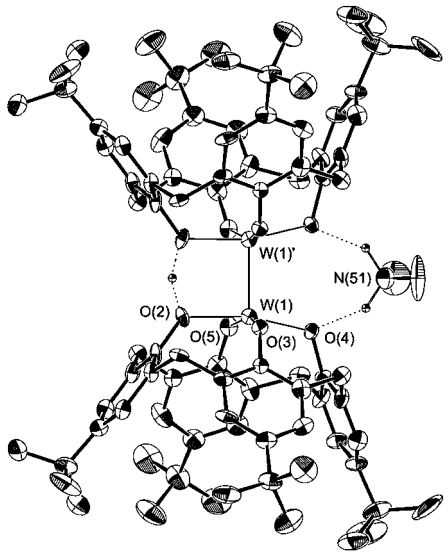

Figure 6. ORTEP drawing of **4**·7PhH (M = W), with the atom-numbering scheme, showing the coordination geometry of metal atom and hydrogen bonding.

Table 4. Selected Bond Distances (Å) and Angles (deg) for **4**·7HPh (M = W)

W1−W1	2.3039(8)	W1−O2	2.066(6)
W1−O3	1.947(6)	W1−O4	1.973(6)
W1−O5	1.959(6)		
O2···O2	2.338(9)	N51···O4	2.764(9)
W1−W1−O2	90.5(2)	W1−W1−O3	99.6(2)
W1−W1−O4	102.8(2)	W1−W1−O5	98.8(2)
O2−W1−O3	85.1(2)	O2−W1−O4	166.7(3)
O2−W1−O5	86.5(2)	O3−W1−O4	92.1(2)
O3−W1−O5	159.8(3)	O4−W1−O5	91.9(2)

correlated with the known structure of **1** (M = Mo) in the solid state (Figure 1). At low temperatures (−20 °C and below) in toluene-d_8, there are four aromatic CH singlets, two sets of diastereotopic methylene signals, and two ^{t}Bu singlets of equal integral intensity. This is consistent with phenyl groups being disposed in and out as described earlier and also is consistent with the μ,η^2,η^2-L bonding mode, which generates two sets of CH_2 groups. Also of note are the $H_2NMe_2^+$ methyl protons at δ ~1.0 ppm. Upon an increase in temperature, the two ^{t}Bu resonances broaden and coalesce at +20 °C and then sharpen to give one ^{t}Bu signal at +40 °C and above. Simultaneously, the aromatic CH resonances collapse in a pairwise manner to give two singlets of equal intensity at higher temperatures. This is consistent with the phenyl groups of the calix[4]arene ligand opening and closing rapidly on the NMR time scale. Notably, the methylene proton resonances are unaffected by these changes, indicating that the central M_2O_8 skeleton is rigid on the NMR time scale. The methyl signal of the $H_2NMe_2^+$ cation remains upfield at δ ~1.0 ppm, indicating that it remains inside the bowl. Also, upon the addition of a large excess of $HNMe_2$ (>10 equiv), the signals for free $HNMe_2$ at δ 2.16 ppm and for encapsulated $H_2NMe_2^+$ at δ 0.55 ppm (20 °C, toluene-d_8, 300 MHz) remain quite distinct. Thus exchange of $H_2NMe_2^+$ within the calix[4]arene bowl and free $HNMe_2$ is slow on the NMR time scale. These findings complement the chemical observations that compounds **1** are not converted to **3** upon heating in solution or under a dynamic vacuum. Note also that if rearrangement of the μ,η^2,η^2-L ligand to the η^4-L geometry occurred in the presence of free amine, then insoluble compounds, $(H_2NMe_2)_2[M_2(\eta^4\text{-L})_2]$, would be formed as evidenced by the fact that **3** and $HNMe_2$ react in this manner.

Compounds **1** show ν(NH) at 3122 cm^{-1} (M = Mo) and 3125 cm^{-1} (M = W) in the infrared spectrum.

Compounds **2** (see Figure 3) show simpler NMR spectra, namely one CH_2 group with diastereotopic protons and one aromatic CH resonance. The HN*Me*$_2$ resonance is at δ ~1.6 ppm and the O*H* or N*H* proton resonance is at δ ~8.5 ppm. The ^{1}H signals associated with pyridine occur at positions consistent with free pyridine, and in the infrared spectrum there is no band above 3046 cm^{-1} assignable to ν(NH or OH). The addition of free $HNMe_2$ leads to only one time-averaged signal for the HN*Me*$_2$ groups, indicative of rapid and reversible binding to the M_2 center. This is consistent with the fact that heating under a dynamic vacuum gives rise to loss of pyridine and $HNMe_2$ to give the compounds **3**.

Compounds **3** show very simple spectra, consistent with the dumbbell-like structure shown in Figure 4, namely one type of ^{t}Bu resonance, a singlet for the aromatic CH protons, and one set of diastereotopic methylene proton signals. The hydroxyl protons are found as a broad resonance at δ ~11 ppm. Again, in the infrared spectrum, there is no evidence for ν(OH) above the aromatic ν(CH) band at 3053 cm^{-1}. The NMR data for the OH group are consistent with an OH···O interaction across the M−M triple bond as seen in $Mo_2(O^iPr)_4(HO^iPr)_4$.[16]

Compound **4** also shows a simple NMR spectrum with only one type of η^4-L ligand, thereby indicating that the hydrogen bonds seen in the solid-state structure (Figure 6) are being formed and broken rapidly. The HN*Me*$_2$ resonance at δ ~1.5 ppm is notably different from that of free $HNMe_2$, which suggests that it is bonded across the W_2 center. Downfield at δ ~12.9 and 8.7 ppm, there are two signals in the integral ratio 1:2 assignable to the OH and NH_2 moieties, respectively, that bridge the W−W triple bond.[18] In the infrared spectrum, once again, no band above 3053 cm^{-1} is observed. Thus only in **2** do we seen clear evidence of the NH_2 protons. In all other compounds, the presence of NH···O, NH···N, or OH···O

(18) The deshielding influence of M−M triple bonds is well established for H atoms lying over the M−M bond. See: Blatchford, T. P.; Chisholm, M. H.; Huffman, J. C. *Polyhedron* **1987**, *6*, 1677.

Table 5. Summary of Crystal Data

	1·4THF (M = Mo)	**2**·4Py (M = Mo)	**3**·*x*HPh (M = Mo)	**4**·7HPh (M = W)
empirical formula	$C_{106}H_{148}Mo_2N_2O_{11.5}$	$C_{112}H_{140}Mo_2N_6O_8$	$C_{100}H_{118}Mo_2O_8$	$C_{132}H_{155}N_1O_8W_2$
color of crystal	dark green	amber	brown	green
crystal dimens (mm)	0.10 × 0.30 × 0.30	0.08 × 0.25 × 0.25	1639.82	0.25 × 0.30 × 0.30
space group	$P2_1$	$P2_1/n$	Immm	Pnma
temp (°C)	−169	−168	−169	−168
a (Å)	13.105(4)	12.384(2)	17.89(2)	25.421(3)
b (Å)	18.631(6)	22.130(3)	18.14(2)	34.611(3)
c (Å)	20.543(6)	18.621(3)	29.15(2)	13.113(1)
β (deg)	94.04(2)	100.26(1)		
Z (molecules/cell)	2	2	4	4
V (Å^3)	5003(3)	5022(1)	9457(14)	11537(2)
d_{calcd} (g cm^{-3})	1.212	1.25	1.152	1.296
wavelength (Å)	0.710 69	0.710 69	0.710 69	0.710 69
mol wt	1826.23	1890.26	1639.82	2251.36
linear abs coeff (cm^{-1})	0.308	0.308	0.317	2.051
detector to sample dist (cm)	22.5	22.5	22.5	22.5
sample to source dist (cm)	23.5	23.5	23.5	23.5
av ω scan width at half-height	0.25	0.25	0.25	0.25
scan speed (deg/min)	6.0	6.0	6.0	10.0
scan width (deg + dispersion)	2.0	1.8	2.0	1.4
indiviual background (s)	6	6	6	3.0
aperture size (mm)	3.0 × 4.0	3.0 × 4.0	30 × 4.0	3.0 × 4.0
2θ range (deg)	6−45	6−45	6−45	6−50
total no. of reflcns collected	9943	10 086	10 323	16 789
no. of unique intensities	8366	6577	3423	10423
no. of reflns with $F > 3\sigma(F)$	7296	4799	1327	6231
R[a]	0.0658	0.0585	0.154	0.0578
R_w[b]	0.1576	0.0584	0.370	0.0519
goodness of fit for last cycle	1.084	1.248	1.135	1.118
max δ/σ for last cycle	0.419	0.16	0.002	0.06

[a] $R = \sum||F_o| - |F_c||/\sum|F_o|$. [b] $R_w = [\sum w(|F_o| - |F_c|)^2/\sum wF_o2]^{1/2}$ where $w = 1/[\sigma^2(|F_o|)]$.

bonding presumably moves these stretching modes to lower energy.

The ^{1}H NMR spectrum for compound **5**, $Mo_2(\eta^4\text{-L}(1))_2$, is entirely consistent with the presence of the dumbbell structure shown in Scheme 2. For the calix[4]arene ligand, we observed three ^{t}Bu singlets in the integral ratio 2:1:1 and one OMe singlet which appears downfield at δ 5.5, consistent with its presence over the M−M triple bond.[17] There are also two sets of diastereotopic methylene proton signals for the CH_2 ligands. The data are quite inconsistent with the presence of μ,η^2,η^2-L(1) ligands.

Raman spectra were obtained for both bridged, μ,η^2,η^2-L and dumbbell-like isomers, η^4-L, but an assignment of ν(M−M) was not possible.

Spectroscopic data are given in the Experimental Section.

Comments on Reaction Pathways. Several points are worthy of note in this work.

1. In the reactions between $M_2(NMe_2)_6$ and the calix[4]arene ligand, H_4L, the reaction proceeds faster for M = Mo than for M = W. Given that the M−M distance in $M_2(NMe_2)_6$ compounds is longer for M = W than for M = Mo by nearly 0.1 Å,[1] it seems that this rate difference must be due to electronic rather than steric factors. Indeed, we propose that the rate-limiting step is the initial replacement of one NMe_2 ligand by one phenoxide and that this requires an essential component of OH···N bonding with concurrent W−O bond formation. Proton transfer to the W−NMe_2 nitrogen may be disfavored relative to Mo−NMe_2 nitrogen by stronger Me_2N-to-W pπ-to-dπ bonding.[19]

2. In the reaction between $M_2(NMe_2)_6$ compounds and the calix[4]arene ligand, we find no evidence for a compound with one calix[4]arene ligand supported by additional NMe_2 ligands. Thus, the initial M−NMe_2 replacement is followed not only by rapid ring closure but also by activation of the other M−NMe_2 groups to substitution. This contrasts with the substitution behavior of the related biphenols, **C** and **D**, described earlier, which give bridged compounds $M_2(NMe_2)_2$-(O∼∼CH_2∼∼O)$_2$ and $M_2(NMe_2)_2$(O∼∼CHMe∼∼O)$_2$.[11] We ascribe this difference to two factors: (1) The calix[4]arene is a macrocyclic ligand with four acidic hydroxyl groups, which should facilitate rapid replacement (after the initial substrate uptake at the M_2 center) of up to four NMe_2 groups. (2) The geometry of the calix[4]arene bowl allows subsequent attack by the second calix[4]arene ligand more readily than it does the initial attack.

3. The conversion of **1** to **2** in refluxing pyridine and the inertness of **1** to otherwise isomerize and lose $HNMe_2$ to give **3** parallel the reactivity of $M_2(NMe_2)_2$(O∼∼CH_2∼∼O)$_2$ compounds that form kinetically favored bridged isomers which isomerize in refluxing pyridine to give chelate isomers. See eq 4. It seems that an associative process involving pyridine is necessary to bring about the μ,η^2,η^2-L to η^4-L coordination, and presumably this involves the formation of M−O−M bridged intermediates.

4. The circuitous conversion of **1** to **3** via **2** contrasts with the direct formation of **3** in the reactions between $M_2(O^tBu)_6$ compounds and the calix[4]arene ligands in hydrocarbon solvents. Thus, the intimate mechanisms of substitution at the dinuclear centers must differ. The addition of $HNMe_2$ to **3** forms $(H_2NMe_2)_2M_2(\mu^4\text{-L})_2$ compounds which are essentially insoluble in hydrocarbon solvents but are otherwise believed to be closely related to **2** and **4**. Probably there is an extended network of

(19) Enhanced π-bonding to W relative to Mo is based on considerations of overlap with the W 5d orbitals being more diffuse than the Mo 4d orbitals. This is, in part, why metallic bonding is stronger for third-row relative to second-row transition elements, and this is reflected in the heats of sublimation of the elements. See: Cotton, F. A.; Wilkinson, G. *Advanced Inorganic Chemistry*, 5th ed.; John Wiley & Sons: New York, 1989.

O···H−N−H···O bonds between dinuclear units. This notion is supported by the fact that $(H_2NMe_2)_2[W_2(\eta^4\text{-L})_2]$ and $W_2(\eta^4\text{-HL})_2$ react to give **4**.

5. It is interesting to note that mixing **2** and **3** in benzene-d_6 for M = Mo yields only one apparent compound by ^{1}H NMR spectroscopy even for different ratios of **2** and **3**. This indicates facile intermolecular scrambling of hydrogen-bonded species. However, for M = W, mixing **2** and **3** in benzene-d_6 gives a mixture of **3** and **4** (as indicated by ^{1}H NMR spectroscopy) when the concentration of **3** is greater than that of **2**. But, when the concentration of **2** is greater than that of **3**, the NMR behavior parallels that for M = Mo where only one time-averaged set of resonances are observed, indicating rapid proton transfer between the dinuclear species in solution. It is this behavior that favors the isolation of **4** for M = W but not for M = Mo.

6. The encapsulated $H_2NMe_2^+$ cations in compounds **1** almost certainly reflect their formation in the substitution of NMe_2 groups at the M_2 center because the addition of $HNMe_2$ to **3** results in $H_2NMe_2^+$ bridging the dinuclear centers as seen in **3** and **4**.

7. The difference in the reactivity of $H_3L(1)$ with $Mo_2(NMe_2)_6$ and $Mo_2(O^tBu)_6$ is also quite striking. The dimethylated ligand of $H_2L(2)$ in its reactions with $TiCl_4$ to give an η^3-L(1) derivative has been noted before by Floriani and co-workers,[13] but to our knowledge the conversion of L(1) to L by demethylation has not been seen. Possibly in our chemistry the greater basicity of the Me_2N^- ligand relative to $^tBuO^-$ provides a driving force for the formation of Me_3N and the conversion of L(1) to L in reaction 5. However, the details of the mechanism of this process are quite unclear.

Reactivity. Floriani[15b] recently described the activation of N_2 including its reductive cleavage to nitride by dinuclear reduced Nb_2(calix[4]arene) complexes. By contrast the W_2^{6+} and Mo_2^{6+} calix[4]arene complexes are remarkably inert with respect to small unsaturated ligands such as CO, RC≡N, and HC≡CH. This contrasts with the higher reactivity of $M_2(OR)_6$ compounds studied in this laboratory.[20] In part, the lack of reactivity of the compounds reported here reflects the greater steric crowding and the higher coordination numbers of the metal atoms, just as previously we noted that $M_2(OR)_4(O_2CR')_2$ and $M_2(OR)_4(\beta\text{-diketonate})_{12}$ complexes were relatively unreactive.[21] However, the relative inertness of the M≡M calix[4]arene complexes allows one to study reactions involving small molecules that occur very rapidly with the less sterically encumbered $M_2(OR)_6$ compounds, such as reactions with O_2[22] and NO.[23] With both of these reactants, products of M−M bond cleavage are observed, and our preliminary investigations of the reactions involving **1**, **2**, O_2 and NO reveal some interesting features.

First, in solution, the dumbbell-like compounds **3** react significantly faster than the bridged compounds **1**. With O_2, an orange product formulated as $(\eta^4\text{-L})M{=}O$ is formed. With NO, again the reaction is slow (relative to $M_2(OR)_6$ compounds) but occurs more rapidly for **3** than for **1**, leading to nitrosyl products, as evidenced by $\bar{\nu}$(NO) = 1712 and 1652 cm^{-1} (M = Mo), respectively. The detailed nature of these complexes remains to be established.

Floriani[24] recently reported the preparation and characterization of calix[4]arene complexes containing W=W, W≡W, and W^{4-}W bonds as sodium salts. It seemed plausible that compounds of the types **1** and **3** should also be redox active and might be converted to M^{4-}M or M=M containing compounds. However, the compounds show irreversible electrochemical behavior, and we have not been able to establish facile interconversions among M−M triple, quadruple, and double bonds in our systems. Probably the presence of the μ-Na^+ ions is important in the Floriani systems. However, further work on the reactivity of the compounds reported herein is clearly warranted.

Concluding Remarks

This work has revealed the fascinating coordination chemistry involving the calix[4]arene ligand and the M−M triple bonds of Mo and W. Depending upon the starting materials, $M_2(NMe_2)_6$ versus $M_2(O^tBu)_6$, we obtain μ,η^2,η^2-L or η^4-L modes of bonding. The conversion of **1** to **3**, which occurs in refluxing pyridine but does not occur upon heating either in solution or in the solid state, further underscores the intricate aspects of the coordination chemistry of these complexes with $(M{\equiv}M)^{6+}$ cores.

Experimental Section

General Procedures. All syntheses and sample manipulations were carried out under an atmosphere of dry and deoxygenated nitrogen with standard Schlenk and glovebox techniques. Hydrocarbon solvents were distilled under N_2 from Na/benzophenone and stored over 4 Å molecular sieves. Spectra were recorded on a Varian XL-300 (300 MHz) spectrometer in dry and deoxygenated benzene-d_6 or pyridine-d_5. All ^{1}H and ^{13}C NMR chemical shifts are reported in ppm relative to the residual protio impurities or ^{13}C signals of the deuterated solvents. Infrared spectra were obtained from KBr pellets with a Nicolet S10P FT-IR spectrometer. Raman spectra were recorded from KCl disks (ca. 50:50 sample:KCl) with 488.0 and 514.5 nm excitation wavelengths.

Chemicals. The preparations of $M_2(NMe_2)_6$ (M = Mo, W) and $M_2(O^tBu)_6$ (M = Mo, W) have been described previously.[25] The ligand *p-tert*-butylcalix[4]arene was purchased commercially and used as received. The partially methylated *p-tert*-butylcalix[4]arenes $H_3L(1)$ and $H_2L(2)$ were prepared as described previously.[13]

$(H_2NMe_2)_2[Mo_2(\mu,\eta^2,\eta^2\text{-L})_2]$, 1 (M = Mo). The reaction mixture of $Mo_2(NMe_2)_6$ (280 mg, 0.60 mmol) and H_4L (650 mg, 1.00 mmol) in 15 mL of benzene was stirred at room temperature overnight. The volatile components were removed in vacuo, and the residue was suspended in hexanes to give a green precipitate **1** (M = Mo), which was collected and dried in vacuo (yield 685 mg, 90%). Crystals of **1**·4THF (M = Mo) suitable for X-ray analysis were obtained by slow evaporation of a THF solution. Anal. Calcd (found) for $C_{92}H_{120}O_8N_2Mo_2$: C, 70.21 (69.98); H, 7.69 (7.87); N, 1.78 (1.81). ^{1}H NMR (300 MHz, 22 °C, benzene-d_6): aromatic *H*, δ 7.30 (b, 8H), δ 6.94 (b, 8H); Ar_2CH_2, δ 6.47 (d, 4H, J_{H-H} = 12.0 Hz), δ 3.59 (d, 4H, J_{H-H} = 12.3 Hz), δ 3.27 (d, 4H, J_{H-H} = 13.5 Hz), δ 2.89 (d, 4H, J_{H-H} = 13.8 Hz); NH_2, δ 2.87 (b, 4H); CMe_3, δ 1.22 (b, 72H); NMe_2, δ 0.79 (t, 12H). ^{13}C{^{1}H} NMR (125 MHz, 22 °C, benzene-d_6): Ar *C*, δ 167.37 (m), 165.01 (m), 141.73 (m), 141.73 (m), 137.62 (m), 133.57 (m), 131.53 (m), 126.13 (m), 125.52 (m), 124.73 (m); NMe_2, δ 38.81; Ar_2CH_2, δ 35.79; Ar *C*Me_3, δ 34.42; CMe_3, δ 32.39. IR (KBr pellet): 3122 s, 3038 w, 2960 s, 2904 m, 2865 m, 1757 w, 1597 w, 1550 w, 1486 s, 1451 s, 1428 m, 1391 m, 1361 m, 1312 s, 1292 s, 1207 s, 1121 m,

(20) Chisholm, M. H. *J. Chem. Soc., Dalton Trans.* **1996**, 1781.
(21) Chisholm, M. H.; Corning, J. F.; Folting, K.; Huffman, J. C.; Raterman, A. L.; Rothwell, I. P.; Streib, W. E. *Inorg. Chem.* **1984**, *23*, 1027.
(22) Chisholm, M. H.; Folting, K.; Huffman, J. C.; Kirkpatrick, C. C. *Inorg. Chem.* **1984**, *23*, 1021.
(23) R = ^{t}Bu: (i) Chisholm, M. H.; Cotton, F. A.; Extine, M. W.; Kelly, R. L. *J. Am. Chem. Soc.* **1978**, *100*, 3354. (ii) Chisholm, M. H.; Cotton, F. A.; Extine, M. W.; Kelley, R. L. *Inorg. Chem.* **1978**, *17*, 2338. R = ^{t}BuMe$_2$Si: Chisholm, M. H.; Cook, C. M.; Streib, W. E. *Inorg. Chim. Acta* **1992**, *198*−*200*, 63.
(24) Giannini, L.; Solari, E.; Floriani, C.; Re, N.; Chiesi-Villa, A.; Rizzoli, C. *Inorg. Chem*. **1999**, *38*, 1438.
(25) (a) Chisholm, M. H.; Martin, J. D. *Inorg. Synth.* **1992**, *29*, 137. (b) Chisholm, M. H.; Cotton, F. A.; Extine, M. W.; Haitko, D. A.; Little, D.; Fanwick, P. E. *Inorg. Chem.* **1979**, *18*, 2266.

1108 w, 1011.7 w, 972 w, 913 m, 875 m, 828 s, 803 m, 786 m, 764 m, 746 m, 677 m, 632 w, 575 m, 560 m, 543 m, 501 w, 473 m, 432 m, 414 m cm^{-1}. Raman (KCl disk): 1602 s, 1559 w, 1487 s, 1336 s, 1251 m, very strong group of lines at 1120−660, 629 w, 595 w, 585 w, 578 m, 468 w, 457 w, 429 m, 418 w cm^{-1}.

$(H_2NMe_2)_2[Mo_2(\eta^4\text{-}L)_2]$, 2 (M = Mo). (a) The green solution of **1** (M = Mo) (260 mg, 0.17 mmol) in 8 mL of pyridine was refluxed for 0.5 h. The resulting amber solution was cooled and allowed to stand at room temperature overnight to yield amber crystals of **2**·4py (M = Mo) (yield 203 mg, 65%), which were suitable for X-ray analysis. Anal. Calcd (found) for $C_{96}H_{120}O_8N_2Mo_2 \cdot 4C_5H_5N$: C, 71.16 (70.80); H, 7.47 (7.52); N, 4.45 (4.12). ^{1}H NMR (300 MHz, 22 °C, benzene-d_6): py *H*, δ 8.51 (m), 6.93 (m), 6.64 (m); NH_2, δ 8.50 (b, 4H); aromatic *H*, δ 7.24 (b, 16H); Ar_2 CH_2, δ 5.29 (d, 8H, J_{H-H} = 11.1 Hz), δ 3.34 (d, 8H, J_{H-H} = 11.1 Hz); NMe_2, δ 1.57 (s, 12H); CMe_3, δ 1.23 (b, 72H). ^{13}C{^{1}H} NMR (125 MHz, 22 °C, benzene-d_6): py *C*, δ 156.64, 135.58, 123.84; aromatic *C*, δ 150.65, 142.82, 132.31, 125.04; NMe_2, δ 35.44; Ar_2 *C*H_2, δ 34.78; Ar *C*Me_3, δ 34.29; CMe_3, δ 32.10.

(b) Excess $HNMe_2$ (1.4 mmol) was added to the frozen brown solution of **3** (M = Mo) (202 mg, 0.13 mmol) at −196 °C by employing a calibrated gas manifold. After the solution was warmed to room temperature, the yellow precipitate **2** (M = Mo) was collected and dried in vacuo (yield 205 mg, 96%). IR (KBr pellet): 3047 w, 3019 w, 2954 s, 2907 m, 2867 m, 1748 w, 1595 w, 1582 w, 1458 s, 1391 w, 1359 m, 1302 s, 1262 s, 1208 s, 1126 m, 1109 m, 1028 m, 1003 m, 918 m, 888 w, 868 m, 821 m, 799 s, 752 m, 702 m, 675 w, 618 w, 546 m, 505 w, 412 w cm^{-1}. Raman (KCl disk): 1604 s, 1475 s, 1336 m, 1321 s, 1284 m, 1249 m, 1216 m, 1206 m, 1162 w, 1110 w, 1033 m, 1005 m, 992 m, 941 w, 923 s, 858 m, 842 m, 827 m, 788 w, 761 w, 753 w, 701 m, 671 m, 633 vw, 592 m, 547 m, 535 m, 504 vw, 460 w, 430 w, 407 m, 372 m, 352 w, 317 w, 269 w cm^{-1}.

$[Mo_2(\eta^4\text{-}HL)_2]$, 3 (M = Mo). The reaction mixture of $Mo_2(O^tBu)_6$ (202 mg, 0.32 mmol) and H_4L (326 mg, 0.50 mmol) in 10 mL of toluene was stirred at room temperature for 2 days. The volatile components were removed in vacuo, and the residue was suspended in hexanes to give a pale brown precipitate of **3** (M = Mo), which was collected and dried in vacuo (yield 336 mg, 91%). Brown needle crystals were obtained by slow evaporation of a benzene solution. Anal. Calcd (found) for $C_{88}H_{106}O_8Mo_2$: C, 71.24 (71.67); H, 7.28 (7.41). ^{1}H NMR (300 MHz, 22 °C, benzene-d_6): O*H*, δ 10.92 (b, 2H); aromatic *H*, δ 7.09 (b, 16H); Ar_2 CH_2: δ 5.17 (d, 8H, J_{H-H} = 12.3 Hz), δ 3.39 (d, 8H, J_{H-H} = 12.6 Hz); CMe_3, δ 1.12 (b, 72H). ^{13}C{^{1}H} NMR (125 MHz, 22 °C, benzene-d_6): aromatic *C*, δ 150.91, 146.56, 133.14, 125.95; Ar_2 *C*H_2, δ 34.40; Ar *C*Me_3, δ 34.06; CMe_3, δ 31.72. IR (KBr pellet): 3053 w, 3025 w, 2960 s, 2932 m, 2964 m, 2867 m, 1749 w, 1597 w, 1577 w, 1481 s, 1463 s, 1391 w, 1362 m, 1302 m, 1248 m, 1195 s, 1123 s, 1106 m, 1026 w, 982 w, 944 w, 915 m, 871 m, 828 s, 793 m, 754 m, 677 m, 632 w, 598 w, 566 m, 514 w, 426 w cm^{-1}. Raman (KCl disk): 1601 s, 1457 s, 1303 s, 1246 s, 1203 m, 1163 w, 1107 m, 1094 w, 970 w, 945 w, 927 m, 839 m, 817 w, 797 w, 785 w, 760 m, 755 m, 676 m, 646 m, 633 m, 600 m, 558 m, 504 w, 484 m, 476 m, 433 w, 400 m, 353 w, 313 m cm^{-1}.

$(H_2NMe_2)_2[W_2(\mu,\eta^2,\eta^2\text{-}L)_2]$, 1 (M = W). (a) The reaction mixture of $W_2(NMe_2)_6$ (360 mg, 0.58 mmol) and H_4L (649 mg, 1.00 mmol) in 12 mL of benzene was stirred at room temperature overnight. The volatile components were removed in vacuo, and the residue was suspended in hexanes to give a gray precipitate (615 mg; ^{1}H NMR spectrum is very complicated). The light brown solution of 200 mg of the gray precipitate was gently refluxed in 10 mL of benzene for 1 h to give a green solution; after the solvent was stripped in vacuo, the residue was suspended in hexane to yield a green precipitate of **1** (M = W), which was collected and dried in vacuo (yield 174 mg, 63%).

(b) The reaction mixture of $W_2(NMe_2)_6$ (380 mg, 0.60 mmol) and H_4L (648 mg, 1.00 mmol) in 15 mL of benzene was stirred at room temperature for 1 h and then refluxed for 3 h. The volatile components were removed in vacuo, and the residue was suspended in hexanes to give a green precipitate of **1** (M = W), which was collected and dried in vacuo (yield 705 mg, 80%). Anal. Calcd (found) for $C_{92}H_{120}O_8N_2W_2$: C, 63.15 (63.76); H, 6.91 (7.02); N, 1.61 (1.48). ^{1}H NMR (300 MHz, 22 °C, benzene-d_6): aromatic *H*, δ 7.30 (d, 8H, J_{H-H} = 2.4 Hz), δ 6.96 (d, 8H, J_{H-H} = 2.4 Hz); Ar_2 CH_2, δ 6.51 (d, 4H, J_{H-H} = 12.0 Hz), δ 3.60 (d, 4H, J_{H-H} = 12.0 Hz), δ 3.57 (d, 4H, J_{H-H} = 13.5 Hz), δ 3.03 (d, 4H, J_{H-H} = 13.5 Hz); NH_2, δ 2.60 (b, 4H); CMe_3, δ 1.22 (b, 72H); NMe_2, δ 0.67 (t, 12H). ^{13}C{^{1}H} NMR (125 MHz, 22 °C, benzene-d_6): Ar *C*, δ 164.24, 133.17, 126.01, 124.67; NMe_2, δ 38.71; Ar_2 *C*H_2, δ 36.58, 34.06; Ar *C*Me_3, δ 34.37; CMe_3, δ 32.39. IR (KBr pellet): 3125 s, 3035 w, 2958 s, 2905 m, 2868 m, 1754 w, 1598 w, 1553 2, 1469 s, 1449 s, 1392 m, 1362 m, 1314 s, 1297 s, 1206 s, 1125 m, 1107 w, 1011 w, 968 w, 911 m, 872 m, 826 s, 802 m, 790 m, 763 m, 745 m, 676 w, 631 w, 577 m, 557 m, 539 m, 465 w, 427 w, 413 w cm^{-1}.

$(H_2NMe_2)_2[W_2(\eta^4\text{-}L)_2]$, 2 (M = W). (a) The green solution of **1** (M = W) (88 mg, 0.050 mmol) in 5 mL of pyridine was heated to 110 °C for 24 h to yield green crystals, **2**·4py (M = W) (yield 32 mg, 31%), which were suitable for X-ray analysis. Anal. Calcd (found) for $C_{96}H_{120}O_8N_2W_2 \cdot 4C_5H_5N$: C, 65.11 (63.55); H, 6.83 (6.72); N, 4.07 (3.89).

(b) $HNMe_2$ (2.4 mmol) was added to the frozen reddish brown solution of **3** (M = W) (480 mg, 0.29 mmol) at −196 °C by employing a calibrated gas manifold. After the solution was warmed to room temperature, the green precipitate of **2** (M = W) was collected and dried in vacuo (yield 482 mg, 95%). IR (KBr pellet): 3046 w, 3031 w, 2957 s, 2904 m, 2867 m, 1742 w, 1598 w, 1459 s, 1392 m, 1362 m, 1301 s, 1264 s, 1203 s, 1125 m, 1110 m, 1025 w, 945 w, 917 m, 869 m, 823, 799 s, 754 m, 676 m, 587 w, 546 m, 505 w, 414 m cm^{-1}.

$W_2[(\eta^4\text{-}HL)_2]$, 3 (M = W). The reaction mixture of $W_2(O^tBu)_6$ (542 mg, 0.67 mmol) and H_4L (650 mg, 1.00 mmol) in 18 mL of toluene was stirred at room temperature for 1 day. The volatile components were removed in vacuo, and the residue was suspended in hexanes to give a reddish brown precipitate of **3** (M = W), which was collected and dried in vacuo (yield 716 mg, 86%). Anal. Calcd (found) for $C_{88}H_{106}O_8W_2$: C, 63.69 (63.77); H, 6.44 (6.61). ^{1}H NMR (300 MHz, 22 °C, benzene-d_6): O*H*, δ 11.51 (b, 2H); aromatic *H*, δ 7.10 (s, 16H); Ar_2 CH_2, δ 5.14 (d, 8H, J_{H-H} = 12.6 Hz), δ 3.39 (d, 8H, J_{H-H} = 12.0 Hz); CMe_3, δ 1.12 (s, 72H). ^{13}C{^{1}H} NMR (125 MHz, 22 °C, benzene-d_6): aromatic *C*, δ 149.90, 146.61, 133.77, 125.93; Ar_2 *C*H_2, δ 34.44; Ar *C*Me_3, δ 34.09; CMe_3, δ 31.74. IR (KBr pellet): 3053 w, 3025 w, 2960 s, 2929 m, 2905 m, 2871 m, 1745 w, 1601 w, 1578 w, 1479 s, 1464 s, 1417 w, 1395 m, 1363 m, 1300 m, 1246 m, 1197 s, 1125 m, 1105 m, 1028 w, 981 w, 919 m, 887 w, 872 m, 827 m, 795 m, 758 m, 728 w, 693 w, 676 m, 634 w, 601 w, 564 m, 510 w, 428 w cm^{-1}.

$(H_2NMe_2)[W_2(\eta^4\text{-}L)(\eta^4\text{-}HL)]$, 4 (M = W). The reaction mixture of **2** (M = W) (105 mg, 0.060 mmol) and **3** (M = W) (100 mg, 0.060 mmol) in 10 mL of benzene was stirred at room temperature. The green solid gradually dissolved, and the resulting brown solution turned green. After 3 h, the volatile components were removed in vacuo, and the residue was suspended in hexanes to give a pale green precipitate of **4** (M = W), which was collected and dried in vacuo (yield 186 mg, 89%). Recrystallization from benzene afforded green crystals of **4**·7PhH (M = W) suitable for X-ray analysis. Anal. Calcd (found) for $C_{100}H_{106}O_8N_2W_2$: C, 48.50 (48.50); H, 7.90 (7.90); N, 4.78 (4.78). ^{1}H NMR (300 MHz, 22 °C, benzene-d_6): O*H*, δ 12.89 (b, 1H); NH_2, δ 8.70 (b, 2H); aromatic *H*, δ 7.20 (s, 16H); Ar_2 CH_2, δ 5.18 (d, 8H, J_{H-H} = 12.0 Hz), δ 3.42 (d, 8H, J_{H-H} = 12.0 Hz); NMe_2, δ 1.46 (b, 6H); CMe_3, δ 1.19 (s, 72H). ^{13}C{^{1}H} NMR (125 MHz, 22 °C, benzene-d_6): aromatic *C*, δ 153.02, 144.71, 133.22, 125.48; Ar_2 *C*H_2, δ 34.37; NMe_2, Ar *C*Me_3, δ 34.09 (overlap); CMe_3, δ 31.96. IR (KBr pellet): 3053 w, 3025 w, 2960 s, 2932 m, 2904 m, 2867 m, 1742 w, 1630 w, 1601 w, 1476 s, 1464 s, 1392 w, 1362 m, 1301 m, 1259 m, 1204 s, 1123 m, 1107 w, 1030 w, 981 w, 919 m, 869 m, 832 m, 799 m, 758 w, 730 m, 693 w, 671 w, 634 w, 567 w, 549 m, 430 w, 465 w, 430 w, 415 w cm^{-1}.

2 to 3 Conversion. The conversion was performed by placing solid **2** or **2**·*x*py (M = Mo, W) (∼10 mg) in a J. Young NMR tube. The samples were heated to 100 °C for 3 days under a dynamic vacuum. ^{1}H NMR spectra of the resulting brown solids, recorded in C_6D_6, were the same as those of **3** (M = Mo, W).

Reaction of 1 (M = Mo) with O_2. Excess O_2 (2.0 mmol) was added to the frozen green solution of **1** (M = Mo) (152 mg, 1.0 mmol) at −196 °C by employing a calibrated gas manifold. After the solution was warmed to room temperature and stirred for 3 days, the yellow precipitate was collected and dried in vacuo (yield 92 mg). IR (KBr

pellet): 3425 w, 3157 w, 2963 s, 2924 m, 2901 m, 2862 m, 1596 w, 1480 m, 1456 s, 1425 m, 1386 w, 1363 m, 1312 w, 1277 m, 1258 w, 1227 w, 1180 vs, 1122 w, 1106 m, 1025 w, 967 s, 916 m, 869 m, 835 s, 788 s, 761 w, 672 m, 637 w, 558 s, 508 w, 427 m cm^{-1}.

Reaction of 3 (M = Mo) with O_2. Excess O_2 (2.0 mmol) was added to the frozen brown solution of **3** (M = Mo) (142 mg, 1.0 mmol) at −196 °C by employing a calibrated gas manifold. After the solution was warmed to room temperature and stirred for 1 day, the yellow precipitate was collected and dried in vacuo (yield 117 mg). IR (KBr pellet): same as that of the product of reaction of **1** (M = Mo) with O_2.

Reaction of 1 (M = Mo) with NO. Excess NO (2.0 mmol) was added to the frozen green solution of **1** (M = Mo) (150 mg, 1.0 mmol) at −196 °C by employing a calibrated gas manifold. After the solution was warmed to room temperature and stirred for 1 day, the orange precipitate was collected and dried in vacuo (86 mg). IR (KBr pellet): 3435 w, 3167 w, 2957 s, 2900 m, 2865 m, 1695 m, 1652 s, 1595 w, 1458 s, 1392 w, 1361 m, 1297 m, 1263 w, 1194 s, 1123w, 1020 w, 912 w, 871 m, 824 m, 796 m, 760 w, 742 w, 677 w, 618 w, 530 m, 507 m, 460 w, 420 m cm^{-1}.

Reaction of 3 (M = Mo) with NO. Excess NO (2.0 mmol) was added to the frozen brown solution of **3** (M = Mo) (140 mg, 1.0 mmol) at −196 °C by employing a calibrated gas manifold. After the solution was warmed to room temperature and stirred for 3 h, the orange precipitate was collected and dried in vacuo (yield 105 mg). IR (KBr pellet): 3405 w, 3056 w, 3963 s, 2901 m, 2858 m, 1708 vs 1600 w, 1465 s, 1456 s, 1413 w, 1390 w, 1363 m, 1328 w, 1293 m, 1231 m, 1180 s, 1118 m, 1095 m, 1033 w, 970 w, 908 m, 866 m, 823 m, 792 m, 749 m, 675 m, 636 m, 598 w, 570 m, 532 m, 504 w, 434 m cm^{-1}.

Reaction of $Mo_2(NMe_2)_6$ with H_3L (1). The reaction mixture of $Mo_2(NMe_2)_6$ (278 mg, 0.60 mmol) and $H_3L(1)$ (687 mg, 1.00 mmol) in 20 mL of benzene was stirred at room temperature for 5 h and then refluxed for 1 day. The volatile components were removed in vacuo, and the residue was suspended in hexanes to give a yellow precipitate of **2** (M = Mo), which was collected and dried in vacuo (yield 576 mg, 76%). ^{1}H NMR (300 MHz, 20 °C, benzene-d_6): NH_2, δ 7.65 (b, 4H); aromatic *H*, δ 7.25 (b, 16H); Ar_2 CH_2, δ 5.30 (d, 8H, J_{H-H} = 11.1 Hz), δ 3.33 (d, 8H, J_{H-H} = 11.1 Hz); NMe_2, δ 1.65 (s, 12H); CMe_3, δ 1.26 (b, 72H).

[$Mo_2(\eta^4$-L(1))$_2$], 5 (M = Mo). The reaction mixture of $Mo_2(O^tBu)_6$ (504 mg, 0.60 mmol) and $H_3L(1)$ (681 mg, 1.00 mmol) in 30 mL of benzene was stirred at room temperature for 5 days. The volatile components were removed in vacuo, and the residue was suspended in hexanes to give a yellow precipitate of **5** (M = Mo), which was collected and dried in vacuo (yield 553 mg, 72%). ^{1}H NMR (300 MHz, 20 °C, benzene-d_6): aromatic *H*, δ 7.27 (m, 8H), δ 6.90 (s, 4H), δ 6.84 (s, 4H); O*Me*, δ 5.4 (s, 6H); Ar_2 CH_2: δ 5.41 (d, 4H, J_{H-H} = 12.0 Hz), δ 4.95 (d, 4H, J_{H-H} = 12.0 Hz), δ 3.38 (d, 4H, J_{H-H} = 12.0 Hz), δ 3.35 (d, 4H, J_{H-H} = 12.0 Hz); CMe_3, δ 1.44 (s, 36H), δ 0.86 (s, 18H), δ 0.66 (s, 18H).

Reaction of $Mo_2(NMe_2)_6$ with $H_2L(2)$. (a) The reaction mixture of $Mo_2(NMe_2)_6$ (128 mg, 0.25 mmol) and $H_2L(2)$ (343 mg, 0.50 mmol) in 10 mL of benzene was stirred at room temperature for 6 days. The volatile components were removed in vacuo; the residue was the starting materials, as evidenced by ^{1}H NMR spectroscopy.

(b) The reaction mixture of $Mo_2(NMe_2)_6$ and $H_2L(2)$ in toluene was refluxed for 6 days; the products were the starting materials.

(c) The solid mixture of $Mo_2(NMe_2)_6$ and $H_2L(2)$ was heated to 180 °C for 6 days; the products were still the starting materials.

Reaction of $Mo_2(O^tBu)_6$ with $H_2L(2)$. (a) The reaction mixture of $Mo_2(O^tBu)_6$ and $H_2L(2)$ in benzene was stirred at room temperature for 6 days. The volatile components were removed in vacuo; the residue consisted of the starting materials, as evidenced by ^{1}H NMR spectroscopy.

Crystallographic Studies. General operating procedures and a listing of programs have been given previously.[22] A summary of crystal data is given in Table 5.

1·4THF (M = Mo). A crystal of approximately trianglar prism shape was selected from the clusters of crystals and mounted in a nitrogen glovebag with silicone grease, and it was then transferred to a goniostat where it was cooled to −169 °C for characterization and data collection. A systematic search of a limited hemisphere of reciprocal space revealed a primitive monoclinic cell. The only condition observed was $k = 2n$ for $0k0$, which limited the space group selection to $P2_1$ and $P2_1/m$. Several unsuccessful attempts were made to solve the structure in space group $P2_1/m$ using direct methods (MULTAN-78 and SHELXS-86) as well as Patterson map analysis. A chemically sensible solution was obtained when space group $P2_1$ was chosen.

The positions of the molybdenum atoms were obtained from an initial *E* map. The positions of the remaining non-hydrogen atoms were obtained from iterations of a least-squares refinement followed by a difference Fourier calculation. In addition to the molecule of interest, the structure contained THF solvent. Unfortunately, since the sample was dry, some solvent had escaped, making it difficult to refine the occupancies and the correlated thermal parameters. Eventually, two well-ordered THF molecules O105−C109 and O110−C114 were included at full occupancy. A third THF (O115−C119) was refined to half-occupancy (free parameter refinement of sof for this THF is 0.46). At the position of a fourth THF, several peaks were interpreted as two disordered overlapping THF molecules. Free parameter refinement of the sof resulted in 0.57 for O120−C124 and 0.43 for O125−C129. All the THF molecules were constrained by averaging their related C−O and C−C distances. One of the *tert*-butyl groups (C51−C54) had large isotropic thermal parameters and did not refine in the anisotropic form. The bonds and angles for the group were quite reasonable, and a disordered structure was not evident in the difference map. Therefore none was introduced.

In the final cycles of refinement, anisotropic thermal parameters for some additional atoms did not converge to realistic values. Atoms C11, C16, C17, C24, C52−C54, C73, and C74 and the atoms of all of the THF solvent molecules were refined with isotropic thermal parameters. All other non-hydrogen atoms were refined with anisotropic thermal parameters. All of the hydrogen atoms for the calix[4]arene ligands and the H_2NMe_2 cations were generated geometrically and assigned fixed isotropic thermal parameters. No hydrogen atoms were generated for the THF solvents. The largest peak in the difference map was 1.4 e $Å^{-3}$, located 1.1 Å from Mo1.

2·4py (M = Mo). A thin plate crystal that was attached to a glass fiber with silicone grease was transferred to the goniostat, where it was cooled to −168 °C for characterization and data collection.

The structure was solved by using a combination of direct methods (SHELXS-86) and Fourier techniques. The Mo atom and several oxygen and carbon atoms of the calix[4]arene ligand were evident in the best solution. The remaining non-hydrogen atoms were located in iterations of a least-squares refinement followed by a difference Fourier calculation. In addition to the Mo_2 unit of interest, the structure contained two molecules of dimethylamine and four molecules of pyridine (which had been used as a solvent during the recrystallization) per dimer. The asymmetric unit contained one half of the Mo_2 unit, one dimethylamine, and two pyridines. The Mo_2 complex has a crystallographic center of inversion at the midpoint of the Mo−Mo bond. Disorder was observed in two of the *tert*-butyl groups. In the *tert*-butyl group on atom C9, atoms C35, C36, and C37 refined to 57% occupancy and atoms C65, C66, and C67 refined to 43% occupancy; in the *tert*-butyl group on C29, atoms C47, C48, and C49 refined to 100%, 60% and 60% occupancies, respectively, and the two additional atoms C68 and C69 refined to 40% occupancy. In the pyridine molecule that is a "guest" in the cavity, the position of the nitrogen atom was not clear. Two atoms, C60 and C63, had lower isotropic thermal parameters than the other atoms in the ring and were refined as a 50−50% mixture of C and N. Many of the hydrogen atoms were evident in a difference map. It should be noted that both hydrogen atoms on the dimethylamine were located. All hydrogen atoms were introduced with fixed idealized positional parameters and isotropic thermal parameters equal to 1.0 plus the isotropic equivalent of the parent atom. On the disordered atoms, hydrogen atoms were introduced only on the dominant part.

The final cycles of least-squares refinement were carried out with anisotropic thermal parameters on all but the disordered atoms (see above). The final $R(F)$ was 0.059 for 6577 reflections and 568 variables (including the scale factor and an overall isotropic extinction parameter). Data with $F < 3\sigma(F)$ were given zero weight. The largest peak in the

difference map was 1.6 e $Å^{-3}$, near the Mo atom (1.5 Å), and the deepest hole was −0.70 e $Å^{-3}$.

3·*x*HPh (M = Mo). The sample was made up of clusters of needle crystals. The crystals were small and tended to shatter when cleaved. Several attempts to select a single crystal were unsuccessful. However, a needle-shaped crystal of dimensions 0.05 × 0.05 × 0.20 mm was selected from the clusters of crystals, mounted with silicone grease, and then transferred to the goniostat, where it was cooled to −169 °C for characterization and data collection. A systematic search of a limited hemisphere of reciprocal space revealed a *C*-centered monoclinic cell. However, successful attempts were made to solve the structure in the orthorhombic unit cell with space group *Immm* by using direct methods (SHELXS-86) and Fourier techniques.

The positions of the molybdenum atoms and non-hydrogen atoms from the calix[4]arene ligand were obtained from an initial *E* map. The asymmetric unit contains two one-eighth of Mo_2 centers in which one is composed of a quarter of a Mo atom, a full butylphenyl ring, and two halves of methylene carbon atoms while the other is composed of a quarter of a Mo atom, two halves of a butylphenyl ring, and one methylene carbon atom. Disorder was observed in all *tert*-butyl groups of the calix[4]arene ligands, and the disordered carbon atoms were refined to 50:50 occupancy. Unfortunately, the crystal was too small and the crystallographic data were not good enough to locate all benzene solvents from iterations of a least-squares refinement followed by a difference Fourier calculation. Hydrogen atoms were introduced in fixed idealized positions with isotropic thermal parameters.

The final cycles of least-squares refinement were carried out with anisotropic thermal parameters on all but the disordered atoms. The final $R(F)$ was 0.159 for 1327 observed reflections ($F > 3\sigma(F)$). Attempts to improve the refinement result were unsuccessful. We only offer these data as support for the gross structural features of the dumbbell-like geometry as demanded by NMR solution data.

4·7HPh (M = W). The green crystals were quite air sensitive and were handled in a nitrogen atmosphere glovebag during crystal selection and mounting. The crystal used for characterization and data collection at −168 °C was a triangular prism cleaved from a larger conglomeration of crystals.

The structure was solved by a combination of direct methods (MULTAN-78) and Fourier techniques. The unique W atom and several atoms from the calix[4]arene ligand were located in the initial *E* map. The remaining non-hydrogen atoms were located in iterations of least-squares refinement followed by a difference Fourier calculation. The asymmetric unit was found to contain one half of the W_2 unit, one molecule of dimethylamine located in a mirror plane, two full molecules of benzene, and three half-molecules of benzene solvent, each situated across a mirror plane. The W_2 complex is located on a crystallographic mirror plane, with the mirror at the midpoint of the W−W bond. Disorder was observed in the *tert*-butyl group on C22 where atoms C43 and C50 refined to 66 and 44% occupancies, respectively. Many hydrogen atoms were evident in a difference map after initial refinement. Hydrogen atoms were introduced in fixed idealized positions with isotropic thermal parameters equal to 1.0 plus the isotropic equivalent of the parent atom. The hydrogen atoms on the dimethylamine were not located. A peak of 0.75 e $Å^{-3}$ was located in the mirror plane between O2 and O2′ in a position that is plausible for the expected hydrogen atom, H84.

The final cycles of least-squares refinement were carried out with anisotropic thermal parameters on all but three atoms: C50, the minor component of the disorder (see above), and atoms C18 and C31, which did not converge well to the anisotropic form. The final difference map contained a peak of 2.7 e $Å^{-3}$ on the mirror plane halfway between the two tungsten atoms. The deepest hole was −1.0 e $Å^{-3}$, in the same section.

Acknowledgment. We thank the National Science Foundation for financial support and Professor R. J. H. Clark and Dr. Stephen Firth for obtaining the Raman spectra.

Supporting Information Available: X-ray crystallographic files, in CIF format, for the four structures reported here. This material is available via the Internet at http://pubs.acs.org. Crystallographic data for **1**·4THF (M = Mo), **2**·4py (M = Mo), and **4**·7HPh (M = W) have been deposited with the Cambridge Crystallographic Data Base. Full crystallographic data are also available from the Reciprocal Data Base via the Internet at URL http://www.iumsc.indiana.edu. Request data and files for No. 97055 for **1**·4THF (M = Mo), No. 97056 for **2**·4py (M = Mo), and No. 97064 for **4**·7HPh (M = W).

IC990513A